Chemosphere xxx (xxxx) xxx

Contents lists available at ScienceDirect

Chemosphere

journal homepage: www.elsevier.com/locate/chemosphere

Natural radionuclides and assessment of radiological hazards in MuongHum, Lao Cai, Vietnam

Nguyen Thanh Duong [a], Duong Van Hao [b, *], Van Loat Bui [c], Duc Thang Duong [d], Trong Trinh Phan [e, g, h], Hoan Le Xuan [f]

[a] Hanoi University of Mining and Geology, No 18, Vien Street, Bac Tu Liem District, Hanoi, Viet Nam
[b] Institute of Research and Development, Duy Tan University, Danang, 550000, Viet Nam
[c] Faculty of Physics, VNU University of Science, 334 Nguyen Trai, Hanoi, Viet Nam
[d] Institute for Nuclear Science and Technology, Vinatom, 179 Hoang Quoc Viet, Hanoi, Viet Nam
[e] Institute of Geological Sciences, Vietnam Academy of Science and Technology, Viet Nam
[f] Radioactive & Rare Minerals Division, Xuan Phuong, Bac Tu Liem, Hanoi, Viet Nam
[g] Graduate University of Science and Technology, Vietnam Academy of Science and Technology, Hanoi, Viet Nam
[h] Royal Academy for Overseas Sciences, Brussels, Belgium

HIGHLIGHTS

- Very high ^{226}Ra, ^{238}U, ^{4} K, and ^{232}Th (^{228}Ra) activity concentrations in Vietnam.
- The radionuclides concentrations show a large variation ratios.
- The difference radioactive concentration between ore bodies and surrounding.
- Strong positive correlation between ^{232}Th activity and total absorbed dose rate.
- The radiological hazard indices far exceed the global average values.

ARTICLE INFO

Article history:
Received 10 June 2020
Received in revised form
3 October 2020
Accepted 16 October 2020
Available online xxx

Handling Editor: Martine Leermakers

Keywords:
Natural radionuclides
Radiological hazard
Rare earth mine
High radioactivity
Disequilibrium
Positive correlation

ABSTRACT

^{226}Ra, ^{238}U, ^{4} K, and ^{232}Th (^{228}Ra) activity concentrations of 61 soil samples distributed surrounding the rare earth element mine (NORM), MH, Lao Cai, Vietnam have been measured by HPGe detector. The activity concentrations of ^{226}Ra, ^{238}U, ^{4} K, and ^{232}Th (^{228}Ra) range from 1179 to 6291 Bq/kg, from 1024 to 8351 Bq/kg, from 260 to 3519 Bq/kg, and from 1476 to 35546 Bq/kg in the ore body and from 21.3 to 964 Bq/kg, from 23.4 to 1635 Bq/kg, from 124 to 3788 Bq/kg, and from 40.9 to 6107 Bq/kg outside the ore body in respective. The study area is considered as the high local natural background radiation with the concentration of ^{226}Ra, ^{238}U, ^{4} K, and ^{232}Th (^{228}Ra) of 156, 254, 647, and 908 Bq/kg in respective. Regarding the spatial distribution, the measured radionuclide concentrations are independent of the distance from measured points to the ore body. With regard to the hazard indices, the average calculated radiological hazard indices, including absorbed gamma dose rate, effective dose equivalent, and excess lifetime cancer risk significantly exceed the global average values. There is a disequilibrium between ^{238}U/^{226}Ra concentrations in studied soil samples. The results also found that the ^{232}Th (^{228}Ra) concentration and total absorbed gamma dose rate show a strong positive correlation (coefficient of determination, $R^2 = 1$).

1. Introduction

Natural radionuclides account for about 80% of the human effective dose per year (IAEA, 1996). Naturally occurring radionuclides are present in many natural resources (the acronym NORM) which was defined for all naturally occurring radioactive materials where human activities have increased the potential for exposure

* Corresponding author.
E-mail addresses: nguyenthanhduong@humg.edu.vn (N.T. Duong), duongvanhao@duytan.edu.vn (D. Van Hao), buivanloat@hus.edu.vn (V.L. Bui), thangdd@vinatom.gov.vn (D.T. Duong), phantrongt@yahoo.com (T.T. Phan), xuanhoan.kt@gmail.com (H. Le Xuan).

https://doi.org/10.1016/j.chemosphere.2020.128671
0045-6535/

in comparison with the unaltered situation (IAEA, 2003). Therein, the natural radionuclides in the soils, such as ^{226}Ra, ^{238}U, ^{4} K, and ^{232}Th (its progenies) significantly contribute to the outdoor terrestrial natural radiation (UNSCEAR, 2008; Bangotra et al., 2018; El-Taher et al., 2018; Kovács et al., 2013; Nguyen et al., 2016; Nguyet et al., 2018). The radionuclides in soil can be transferred to the plant and accumulated in the human body through edible plants (Al-Masri et al., 2008; Karunakara et al., 2013; Asaduzzaman et al., 2014; Khandaker et al., 2016; Tuo et al., 2017; Azeez et al., 2019; Cengiz, 2019; Ibikunle et al., 2019). Thus, the measurement of natural radionuclides in rock, soil and assessment of radiation hazards have received much attention in the literature, especially in and surrounding the high level of radiation areas (Sengupta et al., 2005; War et al., 2008; Mehra and Singh, 2011; Ramasamy et al., 2013; Charro et al., 2013; Duggal et al., 2014; Stajic et al., 2016; Gbadamosi et al., 2018; Liu and Lin, 2018; Shohda et al., 2018; Thu et al., 2019; Ba et al., 2019; Belyaeva et al., 2019; Birami et al., 2019; Dentoni et al., 2020; Zhu and Shaw, 2000; Van et al., 2020). In general, the distribution of natural radionuclides in soil depends on the characteristics of parent rock and soil (weathering products from parent rock) and it varies from one site to another. Therefore, the concentration of natural radionuclides in a local area should be measured and it is necessary for assessment of human exposure.

In Vietnam, there are distributed some rare earth element (REE) mines, especially in northern Vietnam (Le et al., 2015; Nguyen et al., 2017; Van et al., 2020). In which, MH is one of the largest REE mines in Vietnam, which is located in Bat Xat, the northern province of Lao Cai, Vietnam. This REE mine has an area of about 26.84 km^2 and a total probable reserve of 400.000 tons (Moody, 2013). The MH REE mine includes 9 ore bodies distributed in cohesionless sediments of sand, gravel, and clay with the age of Neogene - Quaternary. The rare earth ore mineral composition in MH mine mainly consists of sustainable heavy minerals in exogenous conditions which is typical for the types of placer ores, including monazite, thorium, oxinite, bastnezite, checchite, smacskite, quartz, manhetite, ilmenite, inmenorutin, zircon, octit, sphen, barite. The content of total rare earth element oxides (TR_2O_3) in mine ranges from 0.78 ÷ 3.02% with an average of 1.45%, thorium from 0.111 ÷ 0.188% with an average of 0.157%, uranium from 0.012 ÷ 0.028% with an average of 0.016% (http://dcxh.gov.vn/tin-tuc-tiem-nang-tai-nguyen-va-phan-vung-trien-vong-quang-dat-hiem-o-tay-bac-viet-nam). In the geological point of view, the MH REE mine is located in the north part of the Fanxipan zone which dominated by Proterozoic rocks is a fragment of the Yangtze Platform in south China (Leloup et al., 1995). The mine is placed within the Red River metamorphic belt which is the southeastern part of the ASRR tectonic element in Northwest Vietnam (Tapponnier et al., 1990). Red River metamorphic belt zone had been variously dated between 2360 and 1960 Ma (Tran, 2001), early 575-430 Ma, 263 to 240 Ma, later stage 40 to 22 Ma, the left lateral movement of the Red River shear zone continued after 19–17 Ma, and a rest phase continued from 12 to 5 (Trinh et al., 2012; Thao et al., 2017; Findlay, 2018; Zelazniewicz et al., 2013; Leloup et al., 1995; Huong et al., 2020). In the northeastern part of the mine, the DNCV metamorphic complex is situated and in the southwestern of the Da River belt (Lien and Pho, 2018). In the tectonic plan, Red River zones present active displacements in Quaternary and continue up to present (Liem et al., 2016; Thanh et al., 2018). This mine was recently reported to have a high radioactive background by unpublished data from the Radioactive & Rare Minerals Division. Therefore, in this study, the natural radionuclides in soil (^{226}Ra, ^{238}U, ^{228}Ra (^{228}Th), and ^{4} K) surrounding this mine will be investigated. Besides, the dose and calculated radiological hazard indices estimation are also assessed based on the measured radiation concentration.

2. Materials and methods

2.1. Materials

In the spring of 2019 (March), sixty-one soil samples from different points surrounding MH mine were taken at the depth of about 10–30 cm from the surface. These sampling points were located on three routes (from route 1 to 3) (Fig. 1). Routes 1, 2, and 3 include 21, 21, and 19 sampling points in respective. A kilogram of each soil sample was collected for this study. The soil samples were then removed from the stone, tree root, and then were put into plastic bags. The soil samples were dried at 120 °C to a constant weight. The dried soil samples also were then milled into powder and similar size with standard samples. The powder was weighed and hermetically packed in plastic cylindrical boxes with 121.2 cm^3 cylindrical geometries with a diameter of 70 mm, a height of 31.5 mm and covered with a plastic lid (without gap inside), to prevent radon escape from the sample the lid-vessel connection is sealed with a gas-proof butyl compound. The sample was sealed for 30 days to reach a secular equilibrium between the radium and its daughter radionuclides. Besides, the study samples were stored more than eight months before starting for those procedures which required the equilibrium between ^{238}U and ^{234}Th in the ^{238}U decay chain.

2.2. Methods

The samples were taken to equilibrium status and activity concentration measurements were performed using a high-resolution detector HPGe with a low background of Ortec™. The analysis was performed using Gamma Vision software. The detector energy resolution is 1.9 keV at the 1.33 MeV ^{60}Co gamma-ray peak. To reduce the radiation inside the lead shield, the detector is shielded by a 10-cm thick old-lead cylinder with a 1 mm cadmium and 1 mm copper inner lining. The soil samples were counted for two days to minimize the statistical counting error and activity calculation and calibration were carried out based on standard reference materials (reference materials RG produced by IAEA and IAEA-375).

The activity concentration of each sample was determined based on its respective gamma lines. The gamma lines of 609.3 keV, 1120.3 keV, and 1764.5 keV were used to determine the activity concentration of ^{226}Ra, the gamma line of 1460 keV was used for ^{4} K, and 1001 keV was used for ^{238}U (which was verified by ^{235}U measurement with 186 keV line) while the lines of 911.2 keV, 969.0 keV, 2614.5 keV, 583.0 keV were used for ^{232}Th (^{228}Ra) (there is equilibrium between ^{228}Ra and ^{208}Tl, and the equilibrium between ^{232}Th and ^{228}Ra as the assumption and the really measured radionuclide is ^{228}Ra). The ^{232}Th was mentioned and measured with the assumption of equilibrium between ^{232}Th and ^{228}Ra (^{228}Th) in soil samples (UNSCEAR, 2000; Chiozzi et al., 2002; Atwood, 2013; Khandeker et al., 2016; Stajic et al., 2016; Gbadamosi et al., 2018; Adesiji and Ademola, 2019; Van Hao et al., 2019; Kapanadze et al., 2019; Devi and Chauhan, 2020; Hung and Le, 2020).

The self-gamma absorption resulted from the difference in density of the solid samples and standard ones were introduced following the method described by (Jodlowski, 2006). The activity concentrations of ^{226}Ra, ^{238}U, ^{232}Th (^{228}Ra), and ^{4} K are calculated based on the following formula (Jodlowski and Kalita, 2010) (1)

$$A_{sp} = \frac{N_{sp} M_{st} A_{st} C_i}{N_{st} M_{sp}} \quad (1)$$

Where: A_{sp} and A_{st} are activity concentration of studied and

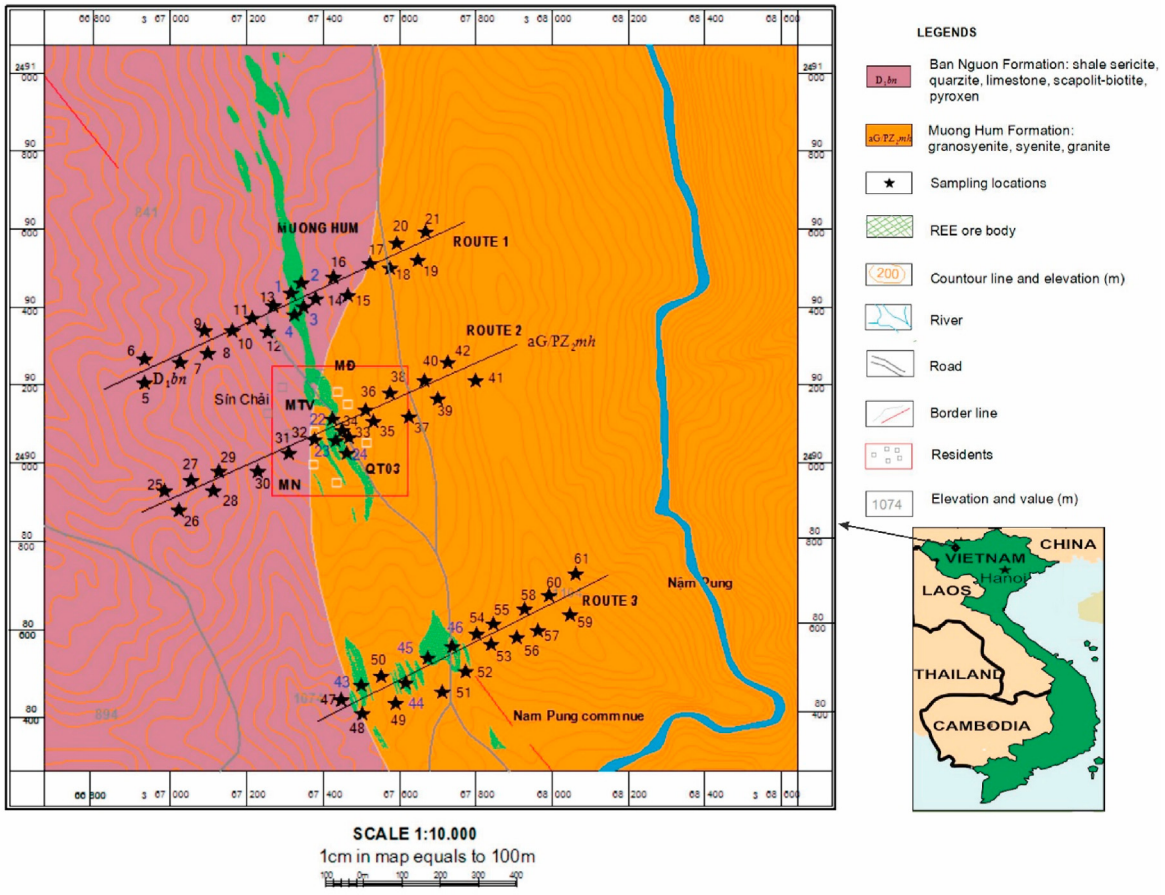

Fig. 1. The sampling points in MH.

standard samples; $\mathbf{N_{sp}}$, $\mathbf{M_{sp}}$, and $\mathbf{N_{st}}$, $\mathbf{M_{st}}$ are the net measured intensity and mass of the sample and standard sample respectively, $\mathbf{C_i}$ - the correction factor for the differences between the densities of the samples and the standard sample.

The Minimum Detection Limit (MDA) of the gamma-ray system is based on the equation taken from (Currie, 1968; Helmer and Debertin, 1988).

$$MDA\ (Bq/kg) = \frac{2,71 + 4,65\sqrt{N_B}}{t \times \varepsilon \times I_\gamma \times M} \quad (2)$$

Where: N_B: is the background counts; t: is the time of measurement (s); ε: is the absolute efficiency of the detector (%); $I\gamma$: is the gamma emission probability; M: is the mass of the sample (kg).

Table 1
Activity concentration of natural radionuclides in soil samples in the ore body.

Sample Nos.	X	Y	Location	^{226}Ra (Bq/kg)	^{238}U (Bq/kg)	^{4} K (Bq/kg)	^{232}Th (^{228}Ra) (Bq/kg)
1	367316	2490438	Ore body	1405	1503	1742	4555
2	367343	2490464	Ore body	3450	6450	644	16179
3	367347	2490403	Ore body	1515	2165	723	2012
4	367324	2490382	Ore body	1325	1024	260	35471
22	367423	2490112	Ore body	1179	1741	900	3640
23	367432	2490059	Ore body	1360	1861	1335	1476
24	367460	2490026	Ore body	1325	1024	260	35471
43	367498	2489433	Ore body	**6291**	**8043**	**2973**	**35546**
44	367616	2489438	Ore body	3812	8351	3519	11011
45	367674	2489503	Ore body	4626	4110	2172	23851
46	367738	2489531	Ore body	2373	2229	1833	21455
Minimum				1179	1024	260	1476
Maximum				6291	8351	3519	35546
Average				2606	3500	1487	17334
Median				1515	2165	1335	16179
Standard Deviation (SD)				1714	2805	1080	13883
Standard Error (SE)				219	359	138	1778
Skewness				1.2	1.0	0.7	0.3
Kurtosis				0.5	−0.7	−0.4	−1.6

2.2.1. Absorbed gamma dose rate

The gamma dose rate, *D*, is used to evaluate the exposure and absorption of radiation to the human body at 1 m above the ground containing naturally occurring radionuclides. The dose rate, *D*, has been evaluated using the conversion factors (absorbed dose rate in the air per unit activity

Per unit of soil mass, (Nano Gray per hour) nGy h^{-1} per Bq kg^{-1}): it equals to 0.46 nGy h^{-1}/Bq kg^{-1} for ^{226}Ra, 0.62 nGy h^{-1}/Bq kg^{-1} for ^{232}Th (^{228}Ra) and 0.042 nGy h^{-1}/Bq kg^{-1} for ^{4} K. Thus, it can be expressed as follows (UNSCEAR, 2000):

$$D\left(nGy.h^{-1}\right) = 0.46A_{Ra} + 0.62A_{Th} + 0.042A_K \quad (3)$$

where, A_{Ra}, A_{Th}, and A_K are activity concentration (Bq/kg) of ^{226}Ra, ^{232}Th (^{228}Ra), and ^{4} K respectively.

2.2.2. Annual effective dose equivalent (AEDE)

The outdoor annual effective dose equivalent (AEDE) was calculated as the following equation:

Table 2
Activity concentration of natural radionuclides in soil samples outside the ore body.

Sample Nos.	X	Y	Location	Distance to the ore body (m)	^{226}Ra (Bq/kg)	^{238}U (Bq/kg)	^{4} K (Bq/kg)	^{232}Th (^{228}Ra) (Bq/kg)
5	366933	2490206	Close ore body	−480 (L1)	141	149	2526	192
6	366932	2490268	Close ore body	−450 (L1)	281	288	1776	441
7	367026	2490259	Close ore body	−310 (L1)	293	425	426	454
8	367089	2490341	Close ore body	−240 (L1)	364	469	1013	871
9	367099	2490283	Close ore body	−220 (L1)	82.1	95.3	510	286
10	367162	2490341	Close ore body	−170 (L1)	34.3	44.4	507	81.9
11	367215	2490372	Close ore body	−110 (L1)	37.0	35.9	384	50.7
12	367255	2490339	Close ore body	−70.0 (L1)	701	933	582	1191
13	367270	2490405	Close ore body	−50.0 (L1)	43.7	41.3	610	82.0
14	367381	2490422	Close ore body	40.0 (R1)	194	202	766	1052
15	367427	2490478	Close ore body	120 (R1)	140	140	260	407
16	367465	2490430	Close ore body	90.0 (R1)	30.3	40.3	341	121
17	367524	2490511	Close ore body	200 (R1)	103	98.0	507	222
18	367576	2490500	Close ore body	250 (R1)	179	190	670	1181
19	367594	2490566	Close ore body	350 (R1)	105	108	435	334
20	367647	2490523	Close ore body	290 (R1)	264	281	233	555
21	367667	2490595	Close ore body	450 (R1)	80.0	83.0	840	160
25	366983	2489929	Close ore body	−490 (L2)	413	353	1585	2685
26	367023	2489882	Close ore body	−420 (L2)	47.2	47.6	133	47.2
27	367053	2489958	Close ore body	−400 (L2)	98.3	92.8	848	160
28	367111	2489930	Close ore body	−300 (L2)	171	292	434	212
29	367126	2489980	Close ore body	−330 (L2)	240	427	518	361
30	367227	2489980	Close ore body	−180 (L2)	166	282	2542	144
31	367310	2490027	Close ore body	−110 (L2)	340	440	1547	240
32	367377	2490062	Close ore body	−20.0 (L2)	964	1635	1692	4503
33	367451	2490084	Close ore body	10.0 (R2)	122	143	3391	204
34	367466	2490067	Close ore body	20.0 (R2)	162	174	2166	257
35	367530	2490107	Close ore body	90.0 (R2)	71.8	65.7	179	51.9
36	367512	2490137	Close ore body	120 (R2)	23.4	23.4	540	151
37	367576	2490180	Close ore body	180 (R2)	25.8	27.8	565	187
38	367625	2490120	Close ore body	140 (R2)	25.0	24.8	562	212
39	367664	2490213	Close ore body	280 (R2)	68.9	66.9	985	159
40	367700	2490165	Close ore body	230 (R2)	81.8	85.0	806	191
41	367728	2490260	Close ore body	420 (R2)	64.9	68.0	946	157
42	367799	2490212	Close ore body	320 (R2)	38.4	53.7	451	104
47	367447	2489393	Close ore body	−30.0 (L3)	34.4	49.5	722	128
48	367503	2489359	Close ore body	−15.0 (L3)	55.8	63.0	358	207
49	367589	2489386	Close ore body	−20.0 (L3)	285	290	3788	1065
50	367711	2489416	Close ore body	−25.0 (L3)	167	270	1272	295
51	367774	2489467	Close ore body	−60.0 (L3)	591	779	258	1300
52	367801	2489563	Close ore body	10.0 (R3)	704	793	643	6107
53	367847	2489588	Close ore body	70.0 (R3)	51.7	33.9	301	90.2
54	367840	2489538	Close ore body	50.0 (R3)	74.8	73.8	240	159
55	367907	2489553	Close ore body	110 (R3)	87.7	92.8	532	547
56	367927	2489626	Close ore body	140 (R3)	55.0	55.2	146	83.9
57	367963	2489571	Close ore body	190 (R3)	65.3	49.6	124	88.9
58	368046	2489611	Close ore body	210 (R3)	54.5	47.8	148	88.7
59	367551	2489455	Close ore body	280 (R3)	**21.3**	**25.1**	**446**	**40.9**
60	368034	2489637	Close ore body	300 (R3)	63.5	45.4	133	84.4
61	368061	2489716	Close ore body	400 (R3)	78.3	70.6	1049	118
Minimum					21.3	23.4	123.8	40.9
Maximum					964	1635	3788	6107
Average					172	213	849	562
Median					85.0	93.0	551	198
Standard Deviation (SD)					199	292	817	1096
Standard Error (SE)					25.0	37.0	105	140
Skewness					2.3	3.0	2.0	3.9
Kurtosis					5.6	11.4	4.0	16.2

L: Left side; R: Right side of the ore body.

$$AEDE\left(\mu Sv.y^{-1}\right) = D\left(nGy.h^{-1}\right) \times DCF\left(Sv.Gy^{-1}\right) \times OF \times T \quad (4)$$

where, D is the absorbed gamma dose rate; DCF is an outdoor dose convention factor (DCF = 0.7 $Sv.Gy^{-1}$); OF is an outdoor occupancy factor (OF = 0.2) (UNSCEAR, 2008); T is the time factor (T = 8760 h).

2.2.3. Excess lifetime cancer risk (ELCR)

Based on the values of AEDE, excess lifetime cancer risks (ELCR) were calculated using the following equations (ICRP, 1990)

$$ELCR = AEDE \times Life\ Expec\tan cy\ (LE) \times Risk\ factor\ (RE) \quad (5)$$

Where LE is the life expectancy of Vietnamese people in North Vietnam and mountainous areas (71 years) (https://www.gso.gov.vn/default_en.aspx?tabid=774); RF is a fatal risk factor per Sievert which is equal to 0.057 Sv^{-1} (ICRP, 1990).

The excess lifetime cancer risk (ELCR) was counted for external gamma radiation only and does not include exposure from inhalation of radon and radon daughters which is a domination exposure component in ordinary residential areas.

3. Results and discussions

3.1. Activity concentration of natural radionuclides in soil

The results of activity concentration of ^{226}Ra, ^{238}U, ^{4} K, and ^{232}Th (^{228}Ra) in and outside the ore body are listed in Tables 1 and 2 in respective. As shown in Table 1, in the ore body, the activity concentrations of ^{226}Ra vary from 1179 to 6291 Bq/kg with an average value of 2606 Bq/kg. The ^{238}U concentration ranges from 1024.4 to 8351 Bq/kg with an average value of 3500Bq/kg. The activity of ^{4} K varies from 260 to 3519 Bq/kg with a mean value of 1487 Bq/kg. While the ^{232}Th (^{228}Ra) concentration ranges from 1476 to 35546 Bq/kg with a mean value of 17334 Bq/kg. Outside the ore body, as presented in Table 2, the concentration of ^{226}Ra, ^{238}U, ^{4} K, and ^{232}Th (^{228}Ra) varied from 21.3 to 964 Bq/kg (172 Bq/kg on average), from 23.4 to 1635 Bq/kg (213 Bq/kg on average), from 124 to 3788 Bq/kg (849 Bq/kg on average), and from 40.9 to 6107 Bq/kg (562 Bq/kg on average) in respective. These results show that the concentration of radionuclides in the ore body is significantly higher than that outside the ore body (close to the ore body). Therein, the concentrations of ^{226}Ra, ^{238}U, ^{4} K, and ^{232}Th (^{228}Ra) in and outside the ore body are significantly higher than the global average concentration in soil in different countries, which are 32 Bq/kg, 33 Bq/kg, 420 Bq/

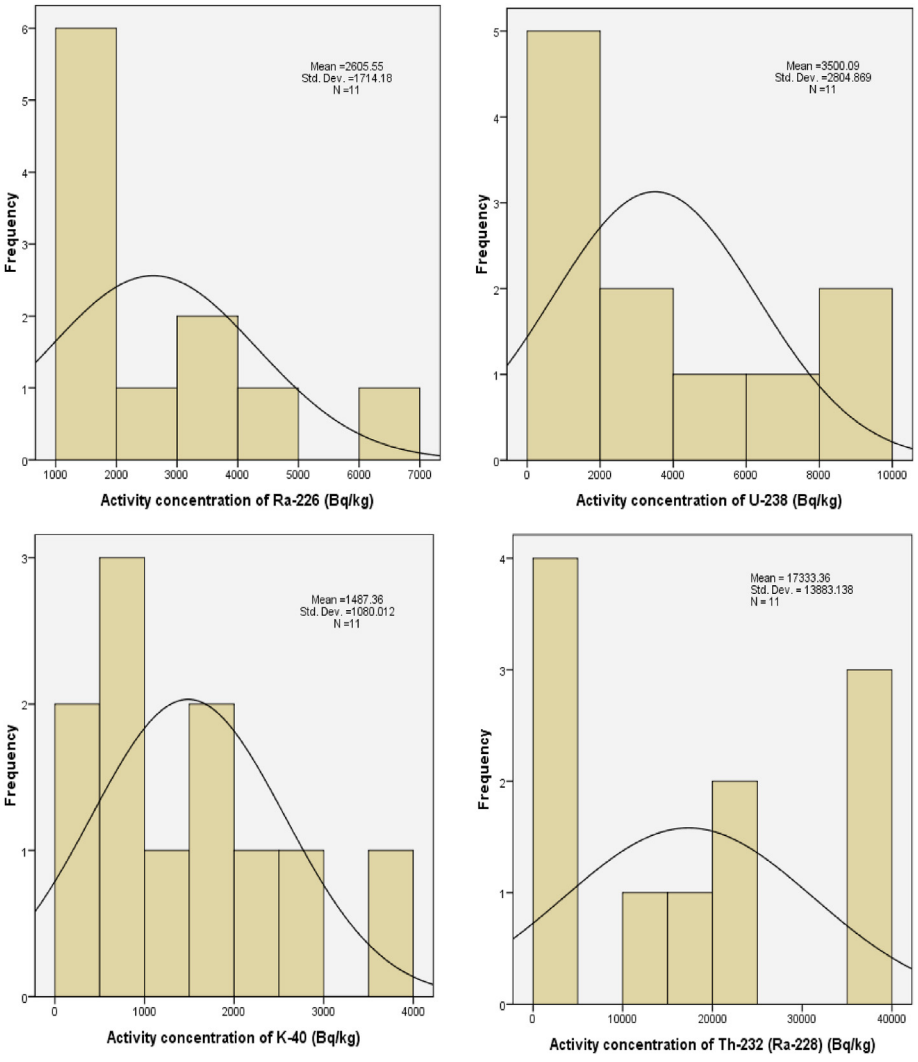

Fig. 2. Distribution curve of ^{226}Ra, ^{238}U, ^{4} K, and ^{232}Th (^{228}Ra) concentrations in the ore body.

kg, and 45 Bq/kg for ^{226}Ra, ^{238}U, ^{4} K, and ^{232}Th (^{228}Ra) respectively (UNSCEAR, 2000). In the ore body, the activity concentrations of ^{226}Ra, ^{238}U, ^{4} K, and ^{232}Th (^{228}Ra) show a large variation with the standard deviation (SD) of 1714, 2805, 1080, and 13883 in respective. In which, the largest variation of activity concentration is found for ^{232}Th (^{228}Ra) while the smallest variation is observed for ^{4} K. By contrast, outside the ore body, the concentration of both ^{4} K and ^{232}Th (^{228}Ra) shows a large variation. The asymmetric distributions of concentrations of measured radionuclides inside and outside the ore body are shown in Figs. 2 and 3. As shown in Fig. 2, in the ore body, the distribution of concentration of ^{226}Ra radionuclide shows the positive Skewness while that of ^{238}U, ^{4} K, and ^{232}Th (^{228}Ra) shows the negative Skewness. In the ore body, the concentration of all studied radionuclides is the light-tailed distribution with the Kurtosis ranging from 0.3 to 1.2. As presented in Fig. 3, the distribution of all studied radionuclides outside the ore body shows the positive Skewness. Additionally, the concentration of ^{226}Ra, these radionuclides is the heavy-tailed distribution (Kurtosis $\geq$3), especially for ^{232}Th (^{228}Ra) radionuclide.

The distribution of concentration of studied radionuclides in three routes concerning the distance from the measurement points to the ore body is presented in Fig. 4. For the three routes, the concentration of ^{232}Th (^{228}Ra) in the ore body is significantly high since the ^{232}Th (^{228}Ra) is the main component of rare earth element mines. Additionally, to both sides of the ore body, the concentration of studied radionuclides (^{226}Ra, ^{238}U, and ^{232}Th (^{228}Ra)) may independent of the distance. It could confirm that the study area without human activities (related REE mine exploring and processing) which non-increase the potential for exposure. Only the ^{4} K have the trend increase in the left side of route 1 and a litter bit high in left side of route 2 (Figs. 6 and 7). It could be explained that the K (^{4} K) is highly mobile and soluble in water (Kumar et al., 2008; FAO, 2016; IAEA, 2014) and to be a greater degree of mobility in comparison with ^{226}Ra, ^{238}U, and ^{232}Th (^{228}Ra) (Hafsi et al., 2014; Kumar et al., 2008), and the left side of route 1, 2 is a low altitude side. Those are the favorable conditions for K (^{4} K) accumulation from leaching due to weathering and erosion from the ore body region. It is not similar for route 3 when the ore body is located in a low altitude zone (Figs. 2 and 8).

The soil samples taken in MH can be assessed as NORM (Naturally Occurring Radioactive Material) because of the study area without human activities related the REE mine. To assess the radioactivity, the local natural background radiation needs to be known. There is no report of the natural background radiation in the study area, so in this study, the authors attempted to determine based on the measured results of radionuclides in soil samples from

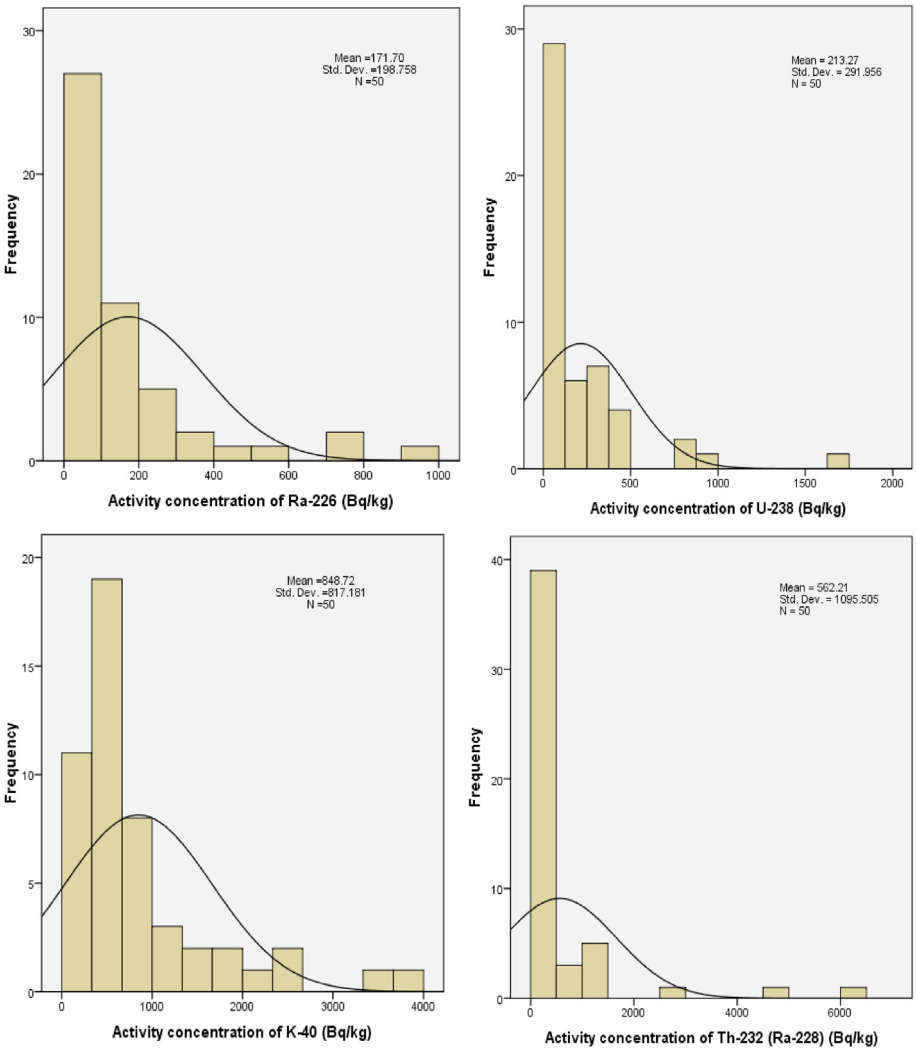

Fig. 3. Distribution curve of ^{226}Ra, ^{238}U, ^{4} K, and ^{232}Th (^{228}Ra) concentrations outside the ore body.

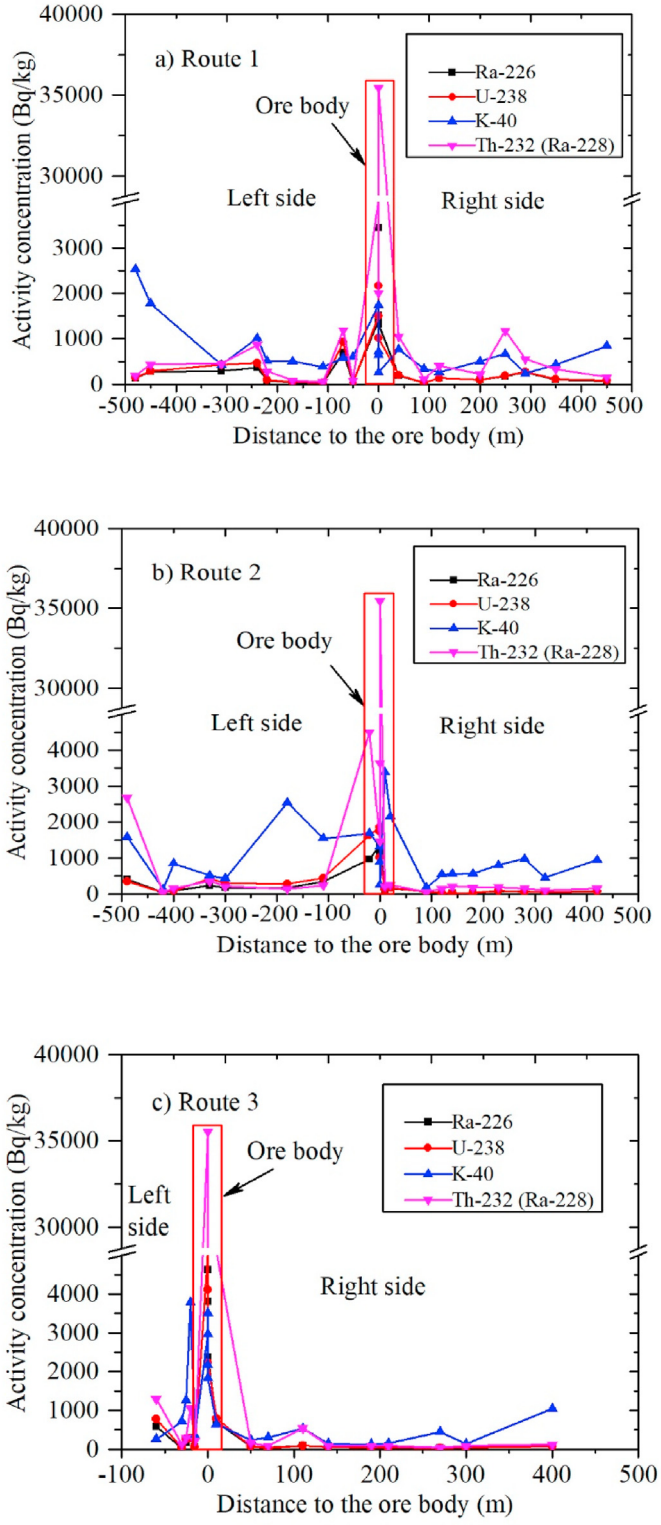

Fig. 4. Variation of radionuclide concentration with distance to the ore body.

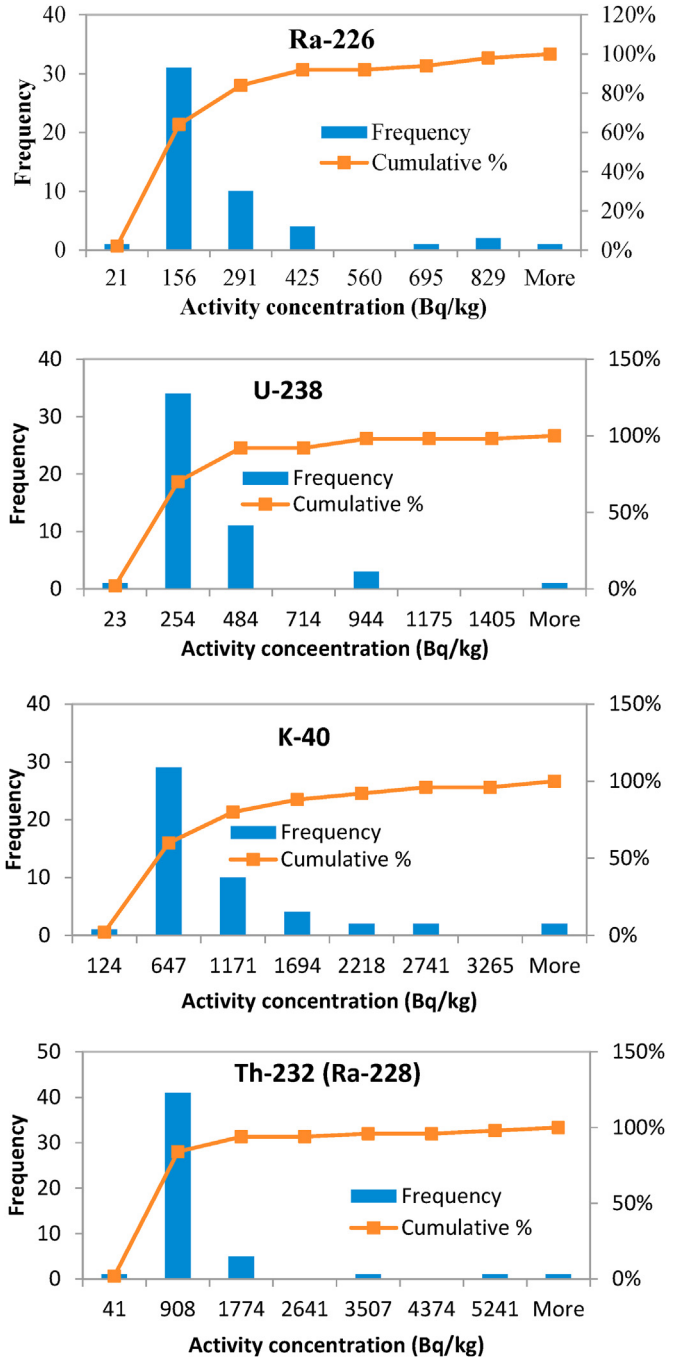

Fig. 5. Frequency and cumulative curve of radionuclide concentration outside the ore body.

inside and outside of ore bodies. Based on the frequency diagram, the local natural background radiation is assumed as the value of concentration having the highest frequency (Son et al., 2014). In this study, the natural background radiation estimated from the concentration of radionuclides in the ore body and close to the ore body is high since the concentration of radionuclides in the ore body is high and not representative. Thus, in the study area, the natural background radiation was estimated from the concentration of radionuclides in soil samples outside the ore body. The frequency diagram of the concentration of radionuclides outside the ore body is plotted and presented in Fig. 5. As shown in Fig. 5, the local natural background radiation of ^{226}Ra, ^{238}U, ^{4} K and ^{232}Th (^{228}Ra) in MH is 156, 254, 647, and 908 Bq/kg in respective. Compared to the average concentration of ^{226}Ra, ^{238}U, ^{4} K, and ^{232}Th (^{228}Ra) in soil in UNSCEAR (2000) (32 Bq/kg, 33 Bq/kg, 420 Bq/kg, and 45 Bq/kg for ^{226}Ra, ^{238}U, ^{4} K, and ^{232}Th (^{228}Ra) respectively), it can be seen that the study area has the high natural background radiation in comparison with average values in soil of other

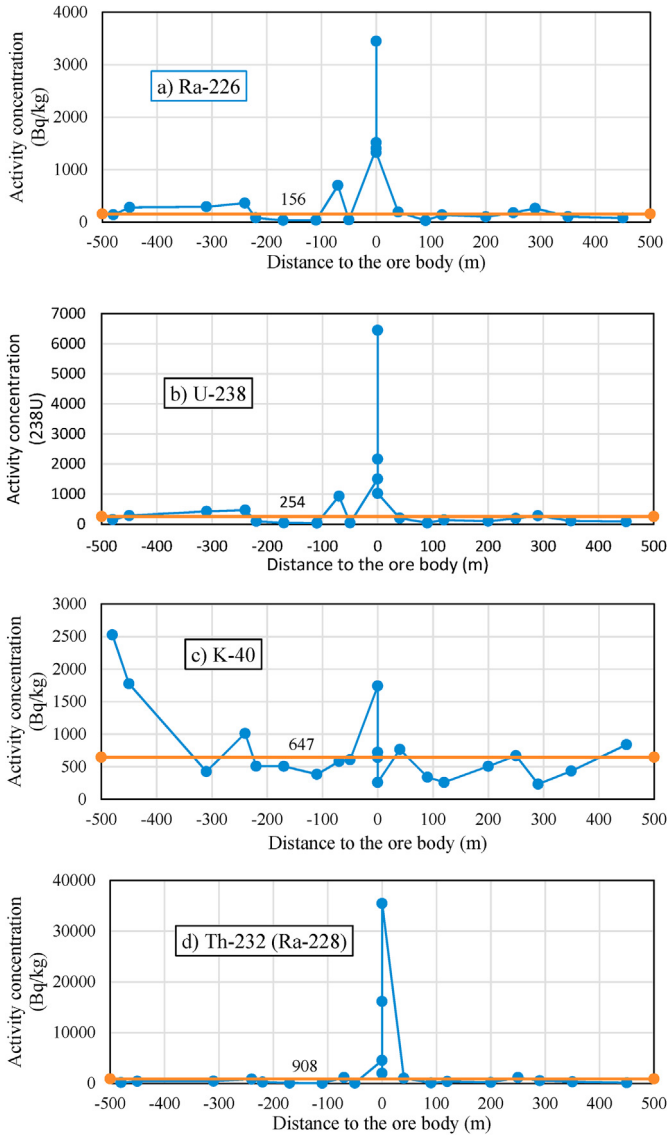

Fig. 6. Natural background radiation and concentration of radionuclides in route 1.

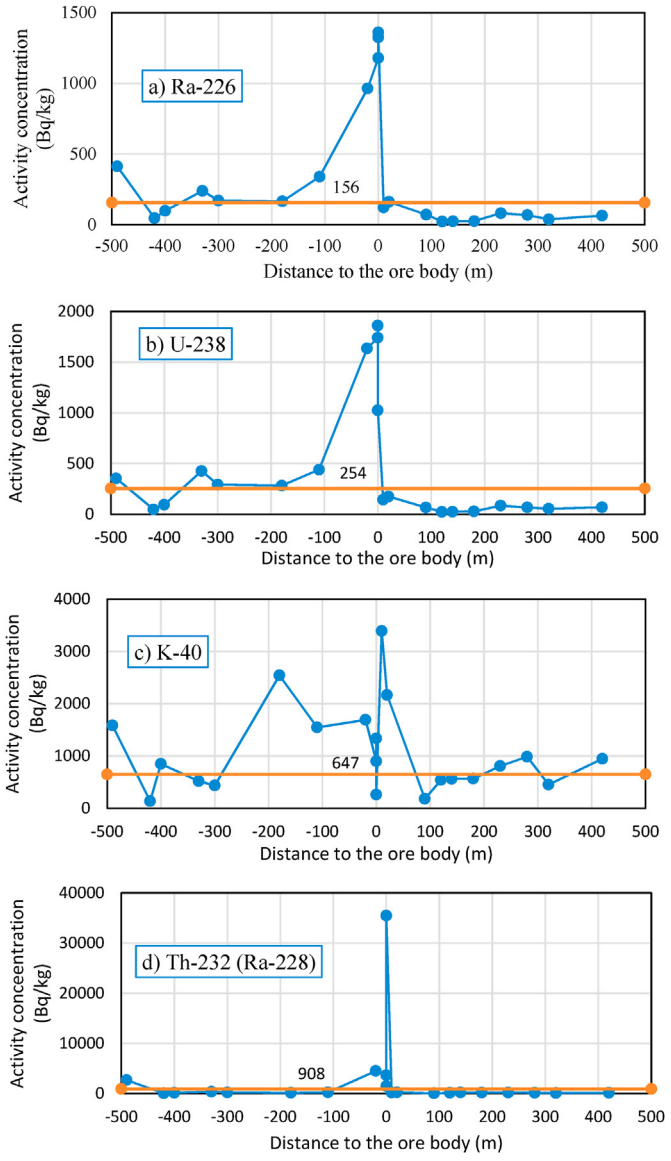

Fig. 7. Natural background radiation and concentration of radionuclides in route 2.

countries in the world.

The comparison of natural background radiation and concentration of radionuclides in soil in three routes is presented in Figs. 6–8. As shown in Fig. 6, the concentration of studied radionuclides in soil samples outside the ore body are fluctuations around the natural background radiation except for ^{4} K which is commented as a light and mobile element (FAO, 2016; IAEA, 2014). In the routes 1 and 2, there are people living and having agricultural activities. However, these activities may not lead to an increase in the radionuclide concentration in soil samples.

For a detailed study, the variation of the concentration ratios ^{238}U/^{226}Ra, ^{232}Th (^{228}Ra)/^{226}Ra, ^{4} K/^{226}Ra, and ^{4} K/^{232}Th (^{228}Ra) and the average values of these ratios are listed in Table 3. In which, the ratio ^{238}U/^{226}Ra slightly ranges from 0.66 to 2.19 with an average value of 1.16. By contrast, the ^{232}Th (^{228}Ra)/^{226}Ra, ^{4} K/^{226}Ra, and ^{4} K/^{232}Th (^{228}Ra) ratios are significantly varied from 0.71 to 27.8, 0.19 to 27.8, and 0.01 to 17.7 with the average values of 3.52, 7.13, and 3.31 respectively. In general, these ratios can be used as a sign of the relative occurrence of these radionuclides in soil. Besides, it is not expected that the concentrations of ^{238}U and ^{226}Ra are in equilibrium. The phenomenon was similar a report of REE mineral for titanium placer in Madagascar by Van Hao et al. (2019). The differences in the mobility of ^{238}U and ^{226}Ra can lead to the difference in concentration of these radionuclides in soil (Navas et al., 2002; Mehra and Singh, 2011). Those differences in the geochemical properties of the uranium and radium elements were mentioned by Van Hao et al. (2019) as well. Thus, the ^{226}Ra occurs in the state of 2+ redox, and ^{226}Ra (Ra element) can be leach by water through various weathering processes while the ^{238}U (U element) could occur in 4+, 5+ and 6+; the other reason is that the ^{238}U series ^{226}Ra is formed after three alpha decays (^{238}U the first), so according to the nuclear recoil ^{226}Ra can be removed from the soil (rock) to the water (rainwater).

3.2. Radiological hazard indices

The summary of the calculated results of radiological hazard indices for the soil in MH area is presented in Table 4. The world average values as reported in UNSCEAR (2000) are also listed in this table.

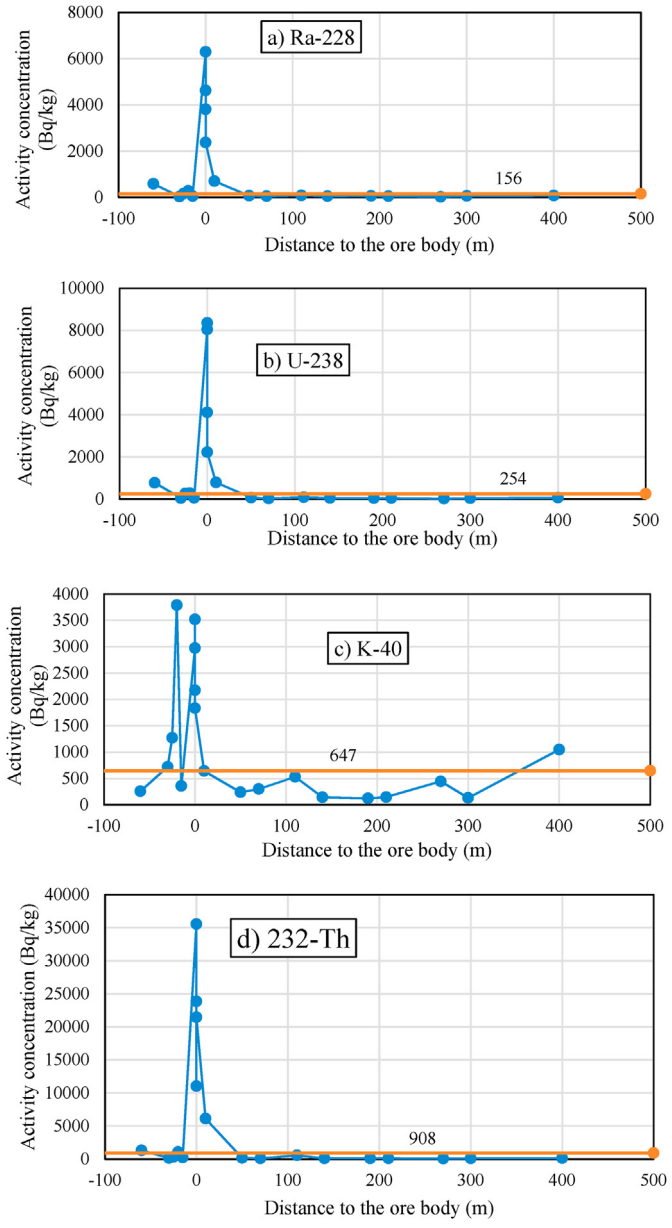

Fig. 8. Natural background radiation and concentration of radionuclides in route 3.

Table 3
Activity concentration ratios $^{238}U/^{226}Ra$, ^{232}Th (^{228}Ra)/^{226}Ra, $^{4}K/^{226}Ra$, and $^{40}K/^{232}Th$ (^{228}Ra).

Values	$^{238}U/^{226}Ra$	$^{232}Th(^{228}Ra)/^{226}Ra$	$^{4}K/^{226}Ra$	$^{4}K/^{232}Th$ (^{228}Ra)
Minimum	**0.66**	**0.71**	**0.19**	**0.01**
Maximum	**2.19**	**27.8**	**27.8**	**17.7**
Average	**1.16**	**3.52**	**7.13**	**3.31**

3.2.1. Absorbed dose rate (D)

The absorbed dose rate shows the received dose in the air at 1 m from the ground of the gamma radiation emitted from the radionuclides in materials in the environment. This parameter is also used to evaluate the health risk. The calculated total absorbed dose rate (D) for soil inside and outside the ore body in MH is ranged from 1597 to 25057 nGy/h with an average value of 12008 nGy/h and from 53.9 to 4138 nGy/h (463 nGy/h on average) respectively (Table 4). It can be seen that the average value of D in the ore body is 26 times higher than that outside the ore body. In the study area, only 2 out of 61 sampling points (Nos. 26 and 59) have the value of D close to the world average value of 57 nGy/h (UNSCEAR, 2000). In general, the average values of D inside and outside the ore body are 211 and 8 times higher than the recommended values in respective. Refer to other countries, the absorbed dose rate values in some areas are also significantly higher than the recommended value such as Chhatrapur, (India) (Mohanty et al., 2004), Bhimilipatanam (India) (Paul et al., 1998), Kerala (India) (Ramasamy et al., 2013), Northern Iran (Birami et al., 2019).

The fractional contributions of natural radionuclides (^{226}Ra, ^{4}K, and ^{232}Th (^{228}Ra)) to the total absorbed dose rate are calculated and presented in Fig. 9. It can be seen that the contributions of radionuclides to the total absorbed dose rate vary from site to site. In most of the sites, the contribution of ^{232}Th (^{228}Ra) to the total dose rate is higher than that of ^{4}K and ^{226}Ra, except the site nos. 31 and 35. This is due to the dominance of ^{232}Th (^{228}Ra) in rare earth element mines (and in the study area in general). In the site no. 31, the contribution of ^{226}Ra (42.3%) is slightly higher than that of ^{232}Th (^{228}Ra) (40.2%) while in the site no. 35, the contributions of ^{226}Ra and ^{232}Th (^{228}Ra) are 45.4% and 44.2% in respective. In general, the contributions of ^{226}Ra, ^{4}K, and ^{232}Th (^{228}Ra) to the total dose rate are 21.2%, 11.8%, and 67.0% respectively. An interesting point as shown in Fig. 10 is that the concentration of ^{232}Th (^{228}Ra) has a very strong correlation with the total dose rate (coefficient of determination, $R^2 = 1$). This indicates that the concentration of ^{232}Th (^{228}Ra) can be used to estimate the total dose rate for the study area.

3.2.2. Annual effective dose equivalent (AEDE) and excess lifetime cancer risk (ELCR)

The calculated AEDE values inside and outside the ore body are varied from 1958 to 30730 μSv/y with an average value of 14726 μSv/y and from 66.1 to 5074 μSv/y with 568 μSv/y on average in respective (Table 4). And the calculated values of ELCR are significantly ranged from 0.008 to 0.124 with an average value of 0.06 for soil samples in the ore body and from 0.0003 to 0.021 with the average value of 0.0023 for soil samples outside the ore body. It is clear that both of the average value of AEDE and ELCR in the ore body is about 26 times higher than that outside the ore body. It can be seen that in the study area, only 2 out of 61 sampling points (Nos. 26 and 59) have the AEDE and ELCR values close to the world average value of 70 μSv/y (UNSCEAR, 2000). The average values of AEDE and ELCR inside and outside the ore body are 210 and 8 times higher than the recommended values respectively (UNSCEAR, 2000).

In general, the radiological hazard indices in this study show a wide range of variation because of the large difference between the inside and outside the ore body. The lowest values of radiological hazard indices were found for the soil sample No. 59 which is located far away from the ore body. While the highest values of hazard indices were observed for the soil sample No. 43 which is located on the ore body. In general, the average values of all the calculated radiological hazard indices for soil samples in the ore body are far higher than those for soil samples outside the ore body and the average values of hazard indices inside and outside the ore body are much higher than the recommended values.

4. Conclusions

The natural radionuclides and assessment of radiological hazards in soil in MH, Lao Cai, Vietnam have been throughout investigated in this study. Based on the measurement results and calculation of radiological hazard indices, some conclusions are drawn as follows:

Table 4
Summary of calculated radiological hazard indices.

Location	Indices	Average	Maximum	Minimum	SD	Skewness	Kurtosis	World average (UNSCEAR, 2000)
Ore body	D (nGy/h)	12008	25057	1597	8538	0.2	−1.6	57
	AEDE (μSv/y)	14727	30730	1958	10982	0.2	−1.6	70
	ELCR	0.060	0.124	0.008	0.044	0.2	−1.6	0.29×10^{-3}
Outside the ore body	D (nGy/h)	463	4138	53.9	754	3.6	14.1	57
	AEDE (μSv/y)	568	5074	66.1	934	3.6	14.1	70
	ELCR	0.0023	0.021	0.0003	0.004	3.6	14.1	0.29×10^{-3}

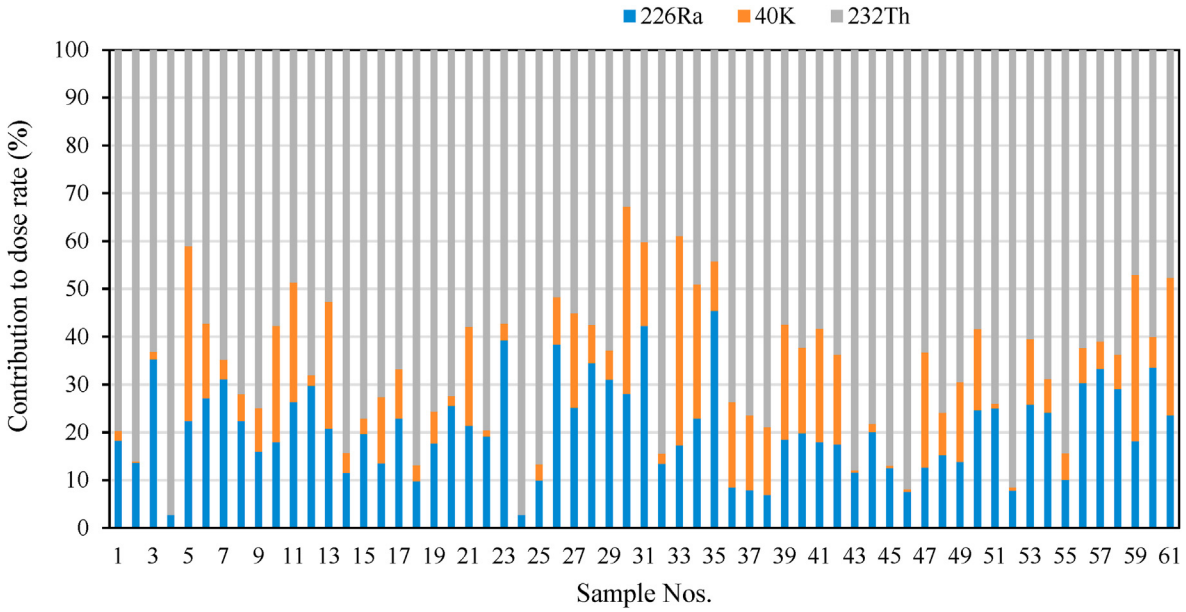

Fig. 9. The fractional contribution of ^{226}Ra, ^{4} K, and ^{232}Th (^{228}Ra) to the total absorbed dose rate.

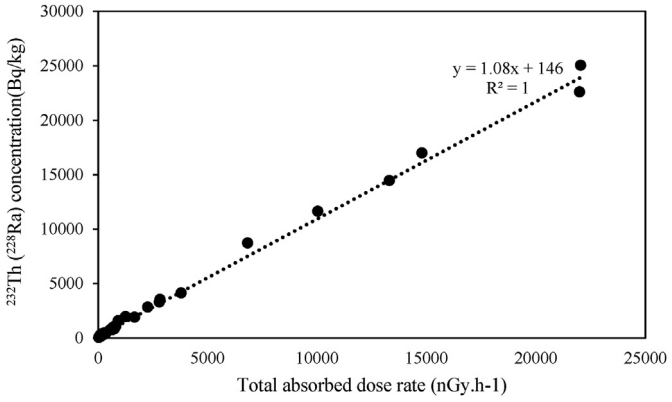

Fig. 10. Relationship between ^{232}Th (^{228}Ra) and total absorbed dose rate.

The research results show that the concentration of radionuclides and calculated radiological hazard indices for soil samples in the ore body are significantly higher than those for soil samples outside the ore body. Additionally, the concentration of radionuclides and radiation hazard indices in and outside the ore body (close to the ore body) is higher than the worldwide average values. Especially in the ore body, the activity concentration of radionuclides is very high in comparison with the average values of those radionuclides in soil of other countries in the world (UNSCEAR, 2000). It should be noted here that the study area has high radiation background. Regarding the spatial distribution, the measured concentration of radionuclides in the study area is independent of the distance from measured points to the ore body, except for the ^{4} K. Since the studied area has a high natural background radiation, the soil samples outside the ore body in MH can be considered as the NORM.

Regarding the disequilibrium among different radionuclides, there are significant variations in the ratios among studied radionuclides and the disequilibrium between ^{238}U and ^{226}Ra. The research also found that the ^{232}Th (^{228}Ra) concentration and the total dose rate has a strong positive correlation. This indicates that the concentration of ^{232}Th (^{228}Ra) can be used to estimate the total dose rate.

Declaration of competing interest

The authors declare that they have no known competing financial interests or personal relationships that could have appeared to influence the work reported in this paper.

References

Adesiji, N.E., Ademola, J.A., 2019. Soil-to-cassava plant transfer factor of natural radionuclides on a mining impacted soil in a tropical ecosystem of Nigeria. J. Environ. Radioact. 201, 1–4.

Al-Masri, M.S., Al-Akel, B., Nashawani, A., Amin, Y., Khalifa, K.H., Al-Ain, F., 2008. Transfer of 40K, 238U, 210Pb, and 210Po from soil to plant in various locations in south of Syria. J. Environ. Radioact. 99, 322–331. https://doi.org/10.1016/j.jenvrad.2007.08.021.

Asaduzzaman, K., Khandaker, M.U., Amin, Y.M., Bradley, D.A., Mahat, R.H., Nor, R.M.,

2014. Soil-to-root vegetable transfer factors for 226Ra, 232Th, 40K, and 88Y in Malaysia. J. Environ. Radioact. 135, 120–127.
Atwood, D.A. (Ed.), 2013. The Rare Earth Elements: Fundamentals and Applications. John Wiley & Sons.
Azeez, H.H., Mansour, H.H., Ahmad, S.T., 2019. Transfer of natural radioactive nuclides from soil to plant crops. Appl. Radiat. Isot. 147, 152–158.
Ba, V.N., Van Thang, N., Dao, N.Q., Thu, H.N.P., Loan, T.T.H., 2019. Study on the characteristics of natural radionuclides in surface soil in Ho Chi Minh City, Vietnam and radiological health hazard. Environmental earth sciences 78, 28.
Bangotra, P., Mehra, R., Jakhu, R., Kaur, K., Pandit, P., Kanse, S., 2018. Estimation of 222Rn exhalation rate and assessment of radiological risk from activity concentration of 226Ra, 232Th and 40K. J. Geochem. Explor. 184, 304–310.
Belyaeva, O., Pyuskyulyan, K., Movsisyan, N., Saghatelyan, A., Carvalho, F.P., 2019. Natural radioactivity in urban soils of mining centers in Armenia: dose rate and risk assessment. Chemosphere 225, 859–870.
Birami, F.A., Moore, F., Faghihi, R., Keshavarzi, B., 2019. Distribution of natural radionuclides and assessment of the associated radiological hazards in the rock and soil samples from a high-level natural radiation area, Northern Iran. J. Radioanal. Nucl. Chem. 322, 2091–2103.
Cengiz, G.B., 2019. Transfer factors of 226 Ra, 232 Th and 40 K from soil to pasture-grass in the northeastern of Turkey. J. Radioanal. Nucl. Chem. 319, 83–89.
Charro, E., Pardo, R., Peña, V., 2013. Chemometric interpretation of vertical profiles of radionuclides in soils near a Spanish coal-fired power plant. Chemosphere 90, 488–496.
Chiozzi, P., Pasquale, V., Verdoya, M., 2002. Naturally occurring radioactivity at the AlpsApennines transition. Radiat. Meas. 35, 147–154.
Currie, L.A., 1968. Limits of qualitative detection and quantitative determination. Anal. Chem. 1968 40 (3), 586–593. https://doi.org/10.1021/ac60259a007.
Dentoni, V., Da Pelo, S., Aghdam, M.M., Randaccio, P., Loi, A., Careddu, N., Bernardini, A., 2020. Natural radioactivity and radon exhalation rate of Sardinian dimension stones. Construct. Build. Mater. 247, 118377.
Devi, V., Chauhan, R.P., 2020. Estimation of natural radionuclide and exhalation rates of environmental radioactive pollutants from the soil of northern India. Nuclear Engineering and Technology 52 (6), 1289–1296.
Duggal, V., Rani, A., Mehra, R., Ramola, R.C., 2014. Assessment of natural radioactivity levels and associated dose rates in soil samples from Northern Rajasthan, India. Radiat. Protect. Dosim. 158, 235–240.
El-Taher, A., Alshahri, F., Elsaman, R., 2018. Environmental impacts of heavy metals, rare earth elements and natural radionuclides in marine sediment from Ras Tanura, Saudi Arabia along the Arabian Gulf. Appl. Radiat. Isot. 132, 95–104.
FAO, 2016. Medium-term Prospects for Raw Materials, Horticulture and Tropical Products. Food and Agriculture Organization of the United Nations (FAO), Rome.
Findlay, R.H., 2018. Geometry, kinematics and regional significance of faulting and related lamprophyric intrusion in the mineralized zone at the Pu Sam Cap complex, Northwest Vietnam. Vietnam J. Earth Sci. 40 (4), 320–340.
Gbadamosi, M.R., Afolabi, T.A., Banjoko, O.O., Ogunneye, A.L., Abudu, K.A., Ogunbanjo, O.O., Jegede, D.O., 2018. Spatial distribution and lifetime cancer risk due to naturally occurring radionuclides in soils around tar-sand deposit area of Ogun State, southwest Nigeria. Chemosphere 193, 1036–1048.
Hafsi, C., Debez, A., Abdelly, C., 2014. Potassium deficiency in plants: effects and signaling cascades. Acta Physiol. Plant. 36, 1055–1070.
Helmer, R.G., Debertin, K., 1988. Gamma-and X-Ray Spectrometry with Semiconductor Detectors. Elsevier Science and Technology.
Huong, N.V., Phong, T.V., Trinh, P.T., Liem, N.V., Thanh, B.N., Pham, B.T., 2020. Recent tectonics, geodynamics and seismotectonics in the ninh thuan nuclear power plants and surrounding regions, south Vietnam. J. Asian Earth Sci. 187, 104080.
Huynh, N.P.T., Le, C.H., 2020. Accumulation rates of natural radionuclides (40K, 210Pb, 226Ra, 238U, and 232Th) in topsoils due to long-term cultivations of water spinach (Ipomoea Aquatica Forssk.) and rice (Oryza Sativa L.) based on model assessments: a case study in Dong Nai province, Vietnam. J. Environ. Manag. 271, 111001.
IAEA, 1996. International Atomic Energy Agency, Vienna.
IAEA, 2003. Extent of Environmental Contamination by Naturally Occurring Radioactive Material (NORM) and Technological Options for Mitigation. International Atomic Energy Agency (Technical Reports series no. 419).
IAEA, 2014. The Environment Behavior of Radium: Revised Edition. International Atomic Energy Agency, Vienna (Technical Reports series no. 476).
Ibikunle, S.B., Arogunjo, A.M., Ajayi, O.S., 2019. Characterization of radiation dose and soil-to-plant transfer factor of natural radionuclides in some cities from south-western Nigeria and its effect on man. Scientific African 3, e00062.
ICRP, 1990. Publication 60. Recommendations of the international commission on radiological protection. Ann. ICRP 21 (1–3).
Jodlowski, P., 2006. Self-absorption correction in gamma-ray spectrometry of environmental samples-an overview of methods and correction values obtained for the selected geometries. Nukleonika 51, 21–25.
Jodlowski, P., Kalita, S.J., 2010. Gamma-ray spectrometry laboratory for high-precision measurements of radionuclide concentrations in environmental samples. Nukleonika 55, 143–148.
Kapanadze, K., Magalashvili, A., Imnadze, P., 2019. Distribution of natural radionuclides in the soils and assessment of radiation hazards in the Khrami Late Variscan crystal massif (Georgia). Heliyon 5 (3), e01377.
Karunakara, N., Rao, C., Ujwal, P., Yashodhara, I., Kumara, S., Ravi, P.M., 2013. Soil to rice transfer factors for 226Ra, 228Ra, 210Pb, 40K and 137Cs: a study on rice grown in India. J. Environ. Radioact. 118, 80–92. https://doi.org/10.1016/j.jenvrad.2012.11.002.
Khandaker, M.U., Nasir, N.L.M., Asaduzzaman, K., Olatunji, M.A., Amin, Y.M., Kassim, H.A., Bradley, D.A., Jojo, P.J., Alrefae, T., 2016. Evaluation of radionuclides transfer from soil-to-edible flora and estimation of radiological dose to the Malaysian populace. Chemosphere 154, 528–536.
Kovács, T., Szeiler, G., Fábián, F., Kardos, R., Gregorič, A., Vaupotič, J., 2013. Systematic survey of natural radioactivity of soil in Slovenia. J. Environ. Radioact. 122, 70–78.
Kumar, A., Singhal, R.K., Preetha, J., Rupali, K., Narayanan, U., Suresh, S., Mishra, M.K., Ranade, A.K., 2008. Impact of tropical ecosystem on the migrational behavior of K-40, Cs-137, Th-232, U-238 in Perennial plants. Water. Air. Soil Pollut 192, 293–302.
Le, K.P., Bui, D.D., Nguyen, D.C., Tibor, K., Nguyen, V.N., Hao, D.V., Nguyen, T.S., Vu, T.M.L., 2015. Estimation of effective dose rates caused by radon and thoron for inhabitants living in rare earth field in northwestern Vietnam (Lai Chau province). J. Radioanal. Nucl. Chem. 306, 309–316.
Leloup, P.H., Lacassin, R., Tapponnier, P., Scharer, U., Zhong, Dalai, Liu, Xiaohan, Zhang, Liangshang, Ji, Shaocheng, Trinh, P.T., 1995. The ailao Shan–Red River shear zone (yunnan, China), tertiary transform boundary of indochina. Tectonophysics 251, 3–84.
Liem, N.V., Trinh, P.T., Vinh, H.Q., Huong, N.V., Quan, N.C., Phong, N.C., Dat, N.P., 2016. Analyze the correlation between the geomorphic indices and recent tectonic active of the Lo River fault zone in southwest of Tam Dao range. Vietnam J. Earth Sci. 38 (1), 1–13.
Lien, N.T., Pho, N.V., 2018. Formation of secondary non-sulfide zinc ore in Cho Dien Pb-Zn deposits. Vietnam J. Earth Sci. 40 (3), 228–239.
Liu, X., Lin, W., 2018. Natural radioactivity in the beach sand and soil along the coastline of Guangxi Province, China. Mar. Pollut. Bull. 135, 446–450.
Mehra, R., Singh, M., 2011. Measurement of radioactivity of 238 U, 226 Ra, 232 Th and 40 K in soil of different geological origins in Northern India. J. Environ. Protect. 2, 960.
Mohanty, A.K., Sengupta, D., Das, S.K., Saha, S.K., Van, K.V., 2004. Natural radioactivity and radiation exposure in the high background area at Chhatrapur beach placer deposit of Orissa, India. J. Environ. Radioact. 75, 15–33.
Moody, M.D., 2013. Mother Lode: the Untapped Rare Earth Mineral Resources of Vietnam. Thesis, Department of Joint Military Operations.
Navas, A., Soto, J., Machin, J., 2002. 238U, 226Ra, 210Pb, 232Th, and 40K activities in soil profiles of the flysch sector (central Spanish pyrenees). Appl. Radiat. Isot. 57 (4), 579–589.
Nguyen, D.C., Le, P.K., Jodłowski, P., Pieczonka, J., Piestrzyński, A., Hao, D.V., Nowak, J., 2016. Natural radioactivity at the sin quyen IOCG deposit in north Vietnam. Acta Geophys. 64 (6), 2305–2321.
Nguyen, D.C., Pieczonka, J., Piestrzyński, A., Hao, D.V., Le, K.P., Jodłowski, P., 2017. General characteristics of rare earth and radioactive elements in dong pao deposit. Lai Chau. Vietnam J. Earth Sci. 39 (1), 14–26.
Nguyet, N.T.A., Duong, N.T., Schimmelmann, A., Huong, N.V., 2018. Human exposure to radon radiation geohazard in rong cave, dong van karst plateau geopark, Vietnam. Vietnam J. Earth Sci. 40 (2), 117–125.
Paul, A.C., Pillai, P.M.B., Haridasan, P.P., Radhakrishnan, S., Krishnamony, S., 1998. Population exposure to airborne thorium at the high natural radiation areas in India. J. Environ. Radioact. 40, 251–259.
Ramasamy, V., Sundarrajan, M., Paramasivam, K., Meenakshisundaram, V., Suresh, G., 2013. Assessment of spatial distribution and radiological hazardous nature of radionuclides in high background radiation area, Kerala, India. Appl. Radiat. Isot. 73, 21–31.
Sengupta, D., Mohanty, A.K., Das, S.K., Saha, S.K., 2005. Natural radioactivity in the high background radiation area at Erasama beach placer deposit of Orissa, India. International Congress Series. Elsevier, pp. 210–211.
Shohda, A.M., Draz, W.M., Ali, F.A., Yassien, M.A., 2018. Natural radioactivity levels and evaluation of radiological hazards in some Egyptian ornamental stones. Journal of radiation research and applied sciences 11, 323–327.
Son, N.T., Phon, L.K., Nam, N.V., Long, L.T., Hao, D.V., Tam, D.V., 2014. Study of methods to determine the local radiation background and increase doses for prospecting activities Nậm Xe deposits, Phong Thổ district, Lai Châu Province. Geol. J. 342–345 (Abstract in English).
Stajic, J.M., Milenkovic, B., Pucarevic, M., Stojic, N., Vasiljevic, I., Nikezic, D., 2016. Exposure of school children to polycyclic aromatic hydrocarbons, heavy metals and radionuclides in the urban soil of Kragujevac city, Central Serbia. Chemosphere 146, 68–74.
Tapponnier, P., Lacassin, R., Leloup, P.H., Schuarer, U., Zhong, D., Wu, H., Liu, X., Ji, S., Zhang, L., Zhong, J., 1990. The ailao Shan/Red River metamorphic belt: tertiary left-lateral shear between indochina and south China. Nature 343, 431–437.
Thanh, N.T., Liu, P.J., Dong, M.D., Nhon, D.H., Dung, B.V., Phach, P.V., 2018. Late Pleistocene-Holocene sequence stratigraphy of the subaqueous Red River delta and the adjacent shelf. Vietnam J. Earth Sci. 40 (3), 271–288.
Thao, H.M., Hien, T.T., Anh, D.D., Nga, P.T., 2017. Mineralogical characteristics of graphite ore from Bao Ha deposit, Lao Cai Province and proposing a wise use. Vietnam J. Earth Sci. 39 (4), 324–336.
Thu, H.N.P., Van Thang, N., Loan, T.T.H., Van Dong, N., 2019. Natural radioactivity and radon emanation coefficient in the soil of Ninh Son region. Vietnam. Applied geochemistry 104, 176–183.
Tran, N.N., 2001. The age of the Ca vinh and xom giau complexes dated by SHRIMP U-Pb analysis of zircon. Vietnam Journal of Geology 1–2, 1–10 [in Vietnamese].
Trinh, P.T., Liem, N.V., Huong, N.V., Vinh, H.Q., Thom, B.V., Thao, B.T., Tan, M.T., Hoang, N., 2012. Late quaternary tectonics and seismotectonics along the Red River fault zone, North Vietnam. Earth Sci. Rev. 114, 224–235.

Tuo, F., Zhang, J., Li, W., Yao, S., Zhou, Q., Li, Z., 2017. Radionuclides in mushrooms and soil-to-mushroom transfer factors in certain areas of China. J. Environ. Radioact. 180, 59–64.

UNSCEAR, 2000. Sources and Effects of Lonizing Radiation. Report to the General Assembly with Scientific Annexes (New York).

Van, H.D., Lantoarindriaka, A., Piestrzyński, A., Trinh, P.T., 2020. Fort-Dauphin beach sands, south Madagascar: natural radionuclides and mineralogical studies. Vietnam J. Earth Sci 42 (2), 118–129. https://doi.org/10.15625/0866-7187/42/2/14951.

UNSCEAR, 2008. Sources and Effects of Ionizing Radiation. Report to the General Assembly with Scientific Annexes. United Nations Scientific Committee on the Effects of Atomic Radiation, New York.

Van Hao, D., Dinh, C.N., Jodłowski, P., Kovacs, T., 2019. High-level natural radionuclides from the Mandena deposit, South Madagascar. J. Radioanal. Nucl. Chem. 319 (3), 1331–1338.

War, S.A., Nongkynrih, P., Khathing, D.T., Iongwai, P.S., Jha, S.K., 2008. Spatial distribution of natural radioactivity levels in topsoil around the high-uranium mineralization zone of Kylleng-Pyndensohiong (Mawthabah) areas, West Khasi Hills District, Meghalaya, India. J. Environ. Radioact. 99, 1665–1670.

Zelazniewicz, A., Tran, H.T., Larionov, A., 2013. The significance of geological and zircon age data derived from the wall rocks of the Ailaoshan-red River shear zone, NW Vietnam. J. Geodyn. 69, 122–139.

Zhu, Y.G., Shaw, G., 2000. Soil contamination with radionuclides and potential remediation. Chemosphere 41, 121–128.